Gas–solid carbonation of Ca(OH)$_2$ and CaO particles under non-isothermal and isothermal conditions by using a thermogravimetric analyzer: Implications for CO$_2$ capture

G. Montes-Hernandez [a,*], R. Chiriac [b], F. Toche [b], F. Renard [a,c]

[a] ISTerre, University of Grenoble I and CNRS, BP 53, 38041 Grenoble Cedex 9, France
[b] Université de Lyon, Université Lyon 1, Laboratoire des Multimatériaux et Interfaces UMR CNRS 5615, 43 bd du 11 Novembre 1918, 69622 Villeurbanne Cedex, France
[c] Physics of Geological Processes, University of Oslo, Norway

ARTICLE INFO

ABSTRACT

The gas–solid carbonation of alkaline sorbents has been actively investigated as an alternative method to CO$_2$ capture from industrial combustion sources and CO$_2$ contained in the air. This study has a two-fold objective: firstly, quantify the gas–solid carbonation extent and the carbonation kinetics of Ca(OH)$_2$ and CaO; and secondly, propose a reaction mechanism of gas–solid carbonation for CaO under dry conditions (relative humidity close to 0), i.e., when the action of water is negligible. The main results of our study have revealed that a high proportion of Ca(OH)$_2$ nanoparticles were transformed into CaCO$_3$ particles by gas–solid carbonation (carbonation extent, $\xi > 0.94$) under non-isothermal conditions. Moreover, this gas–solid reaction requires low activation energy ($E_a \approx 6$ kJ/mol) at a constant heating rate of 5 or 10 K/min. A similar carbonation extent was determined for gas–solid carbonation of in situ synthesized CaO under non-isothermal conditions. However, the gas–solid carbonation of CaO takes place in a broader temperature range, implying a more complex thermokinetic behavior (overlapping of carbonation regimes or steps). Concerning the gas–solid carbonation of Ca(OH)$_2$ and CaO under isothermal conditions, a high carbonation extent (>0.9) was determined for CaO at 600 (873 K) and 800 °C (1073 K). Conversely, the gas–solid carbonation of Ca(OH)$_2$ particles was relatively low (<0.56) at 400 °C (673 K) after 6 h of reaction. This case is in agreement with the formation of a dense non-porous layer of carbonate mineral around the core of the reacting Ca(OH)$_2$ particles, thereby limiting the transfer of CO$_2$.

Finally, an alternative reaction mechanism is proposed for the gas–solid carbonation of CaO, when the relative humidity is close to 0. This macroscopic control at high temperature avoids CO$_2$ dissociation with molecular water at the CaO–CO$_2$ interface. For these specific conditions, the mineralization of adsorbed CO$_2$ on CaO particles implies a solid state transformation, i.e., CaCO$_3$ formation from CaO–CO$_2$ interactions. This could be explained by an atomic excitation than at high temperature allows the local migration of one oxygen atom from the solid toward the adsorbed CO$_2$ leading to its mineralization into carbonate (porous or non-porous layer) around the reacting particles; chemically the mineralization of CO$_2$ also implies the breaking of one covalent bond in the CO$_2$ molecule.

1. Introduction

Gas–solid reactions are ubiquitous in many natural and artificial environments (e.g., instantaneous or slow reactions of volcanic ash, dust and aerosols with natural and/or anthropogenic atmospheric gases). In basic or applied research, gas–solid reactions have been widely used to investigate the oxidation, reduction, chemical vapor deposition, dehydroxylation, carbonation (or mineralization of CO$_2$), decarbonation and other non-limited chemical processes. In particular, there has been growing interest in gas–solid carbonation processes using alkaline sorbents because of their potential to capture CO$_2$ via non-catalytic exothermic reactions, allowing the selective mineralization of CO$_2$ from a complex mixture of several gases (e.g., from industrial combustion processes). Once carbonated, the resulting crystals are then decarbonated at high temperature (with the actual temperature value depending on the nature of the carbonate produced (Prigiobbe et al., 2009; Stendardo and Foscolo, 2009; Zevenhoven et al., 2008; Sun et al., 2008; Shtepenko et al., 2005), releasing pure CO$_2$ by a calcination (or decarbonation) process. Thanks to this overall carbonation–calcination route, pure CO$_2$ can be recovered prior to

* Corresponding author.
E-mail address: german.montes-hernandez@ujf-grenoble.fr
(G. Montes-Hernandez).

its injection underground and reuse, except for carbonates containing monovalent elements (e.g., Na, Li) which volatilize before the decarbonation process. Various alkaline sorbents have been proposed to capture and mineralize CO_2 via gas–solid carbonation such as binary oxides (e.g., CaO, MgO), hydroxides (e.g., $Ca(OH)_2$, $Mg(OH)_2$, NaOH), metastable powdered silicates (e.g., Li_2SiO_3, Na_2SiO_3, $CaSiO_3$, $MgSiO_3$) and natural silicates (e.g., olivine, pyroxene, serpentine) (Larachi et al., 2012; Reddy et al., 2011; Stendardo and Foscolo, 2009; Huntzinger et al., 2009; Regnault et al., 2009; Zevenhoven et al., 2008; Wang et al., 2008; Sun et al., 2008; Gauer and Heschel, 2006; Essaki et al., 2005; Shtepenko et al., 2005; Fernandez Bertos et al., 2004; Lanas and Alvarez, 2004; Purnell et al., 2003). In all cases, the CO_2-sorbent reaction takes place by the formation of a dense non-porous layer of carbonate minerals (or protective carbonate layer) around the reacting particles, to the extent that total carbonation efficiency cannot be achieved (<80%) (e.g., Prigiobbe et al., 2009; Stendardo and Foscolo, 2009; Huntzinger et al., 2009; Sun et al., 2008; Fernandez Bertos et al., 2004), except for cases of high relative humidity (HR > 95%), small particle size (nanometric scale) and nature of sorbent (Zeman, 2008; Seo et al., 2007; Dheilly et al., 2002). The formation of a protective carbonate layer leads to a physical increase in volume at the grain scale (expansion or swelling process) or a decrease in porosity (pore closure process) when porous materials are partially carbonated (Sun et al., 2008; Chen et al., 2007; Fernandez Bertos et al., 2004). With respect to the reaction kinetics, gas–solid carbonation can be catalyzed by water activity (or relative humidity) at moderate temperature (<60 °C) and low CO_2 pressure (<2 bar) (Beruto and Botter, 2000); low water activity (<0.4) ultimately inhibits the reaction (Montes-Hernandez et al., 2010a; Rao et al., 2008). From a mechanistic standpoint, this means that the molecular water adsorbed on hydrophilic and basic surface sites allows carbonate ion formation at the gas–solid interface followed by the formation of solid carbonate around reacting particles. Conversely, for dry gas–solid carbonation (i.e., in the absence of adsorbed water on reacting particles (water activity ≈ 0)), a high temperature (>120 °C) and a preferentially low CO_2 pressure (<1 bar) are required (Montes-Hernandez et al., 2010b). In this case, the optimized reaction temperature depends directly on the textural properties (e.g., particle size, porosity) and chemical nature of absorbent (Zevenhoven et al., 2008; Wang et al., 2008; Fernandez Bertos et al., 2004). Note that the reaction mechanism for dry gas–solid carbonation; i.e., when molecular water action is negligible (water activity ≈ 0), is still a debated question.

The gas–solid carbonation has generally been studied at the laboratory scale by using small reactors coupled with thermogravimetric and/or chromatographic measurements (Blamey et al., 2011; Prigiobbe et al., 2009; Regnault et al., 2009). Conversely, at pilot plant scale, fluidized bed reactors are usually proposed to perform solid–gas carbonation (Reddy et al., 2011; Huntzinger et al., 2009). As previously mentioned, solid–gas carbonation reactions are generally incomplete (<80%) for both cases due to the formation of a protective carbonate layer around the reacting particles. Concerning the gas–solid carbonation of $Ca(OH)_2$ particles, the high relative humidity, the CO_2 pressure and the high temperature (under non-isothermal conditions) can play a crucial role to enable solid–gas carbonation of $Ca(OH)_2$ particles to be completed. For example, Beruto and Botter (2000) clearly demonstrated that an increase in relative humidity catalyzes gas–solid carbonation and increases carbonation efficiency up to 85% at a constant low temperature (≈20 °C) and low CO_2 pressure (≈6.5 mbar). These authors claim that the CO_2 pressure (<1 bar) has a negligible effect on the carbonation process at any relative humidity (<90%). This assumption was later supported by Dheilly et al. (2002). Their study showed that, under certain conditions (atmosphere with low level of CO_2, high relative humidity (RH = 100%) and low temperature

($T = 10$ °C)), the carbonation extent is approximately 93% after 10 days. It reaches 100% after 25 days with a wet hydroxide. Recently, it was demonstrated that $Ca(OH)_2$ nanoparticles can be completely transformed into nanosized calcite (<100 nm) via gas–solid carbonation under moderate CO_2 pressure (<40 bar) and low temperature (<60 °C). For this case, the mineralization of CO_2 does not form the protective carbonate layer around the reacting particles of $Ca(OH)_2$. As a result, the gas–solid carbonation of $Ca(OH)_2$ was more efficient in producing nanosized calcite with high potential for industrial applications (e.g., fillers in the papermaking industry and printing inks, antacid tablets, adsorbents, etc.) (Montes-Hernandez et al., 2010a, 2012). The steam hydration of CaO is typically used to reactivate its performance as a sorbent in calcium looping applications. In this context, Materic et al. (2011) reported that the gas–solid carbonation extent was found to be higher when $Ca(OH)_2$ is directly carbonated at high temperature compared to gas–solid carbonation of CaO, i.e., after $Ca(OH)_2$ dehydration. This relevant insight has also been studied in more detail by Blamey et al. (2011). They investigated the gas–solid carbonation of powder and pellets of $Ca(OH)_2$ and hydrated calcined limestone and dolomite using a thermogravimetric analyzer coupled to a mass spectrometer performing online gas analysis of the off-gas.

This study has a two-fold objective: firstly, quantify the gas–solid carbonation extent and carbonation kinetics of $Ca(OH)_2$ and CaO, and secondly, propose a reaction mechanism of gas–solid carbonation for CaO under dry conditions (relative humidity close to 0), i.e., when the molecular water action is negligible. All carbonation experiments under non-isothermal or isothermal conditions were carried out in a thermogravimetric analyzer where high-purity CO_2 was injected (flow rate = 50 mL/min). For non-isothermal conditions in particular, three heating rates (5, 10 and 20 K/min) were investigated for $Ca(OH)_2$ and a single rate of 10 K/min for CaO. For classic thermogravimetric (TG) analyses and purging steps, 100% N_2 was used in the system.

2. Materials and methods

2.1. Starting reactants

2.1.1. Synthetic portlandite or powdered calcium hydroxide $(Ca(OH)_2)$

Portlandite material or calcium hydroxide $Ca(OH)_2$ was provided by Sigma–Aldrich with 96% chemical purity, with about 3% of $CaCO_3$ and 1% of other impurities. The portlandite material is characterized by platy nanoparticles (sheet forms) forming micrometric aggregates with high porosity and/or high specific surface area (16 m^2/g). The average particle size of 31 nm was deduced from Rietveld refinement of XRD patterns (see Montes-Hernandez et al., 2010b, 2012). For the carbonation experiments, the portlandite was used without any physico-chemical treatment.

2.1.2. Carbon dioxide (CO_2)

Carbon dioxide CO_2 was provided by Linde Gas S. A. with 99.995% chemical purity. This gas was directly injected at a rate of 50 mL/min in the themogravimetric analyzer (small-reaction cell) without any treatment and/or purification.

2.2. Gas–solid carbonation experiments under non-isothermal conditions

All carbonation experiments under non-isothermal conditions were performed with a TGA/SDTA 851[e] Mettler Toledo instrument under the following conditions: sample mass of about 10 mg, alumina crucible of 150 μl with a pinhole, heating rate of 10 °C min^{-1}, temperature range from 30 (303 K) to 1200 °C (1473 K) and 100%
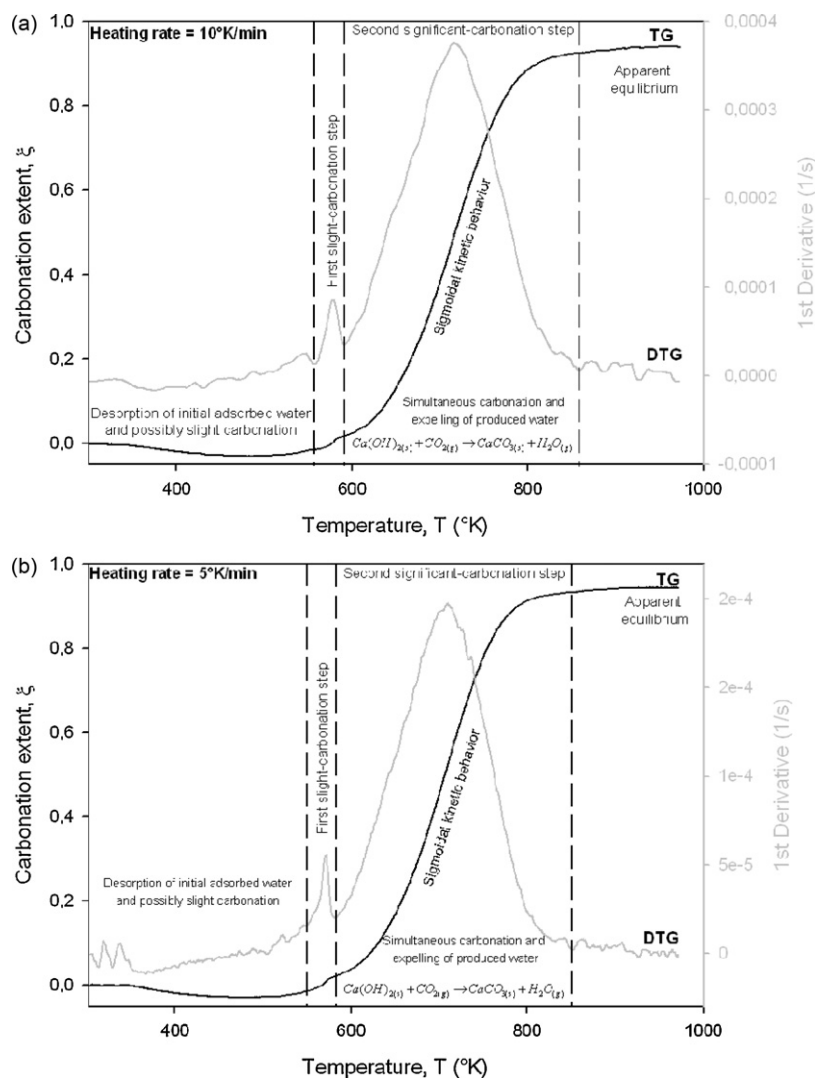
Fig. 1. Gas–solid carbonation of Ca(OH)$_2$ nanoparticles under non-isothermal conditions at two different heating rates (5 and 10 K/min). Carbonation extent (ξ) was determined from thermogravimetric (TG) curves and differential thermogravimetric (DTG) curves were used to identify the carbonation steps and determine the activation energy (see Eq. (2) and Table 1).

CO$_2$ atmosphere of 50 mL min^{-1}. Experiments with additional heating rates of 5 and 20 °C/min were performed for carbonation of Ca(OH)$_2$ particles. Sample mass gain/loss and associated thermal effects were obtained by TGA/SDTA. In order to identify the different mass gain/loss steps, the TGA first derivative (mass gain/loss rate) was used. The TGA apparatus was calibrated in terms of mass and temperature. Calcium oxalate was used for the sample mass calibration. The melting points of three compounds (indium, aluminum and copper) obtained from the DTA signals were used for the sample temperature calibration.

Note that the CaO particles were directly synthesized in the TG analyzer prior to the carbonation experiment as follows: (1) dehydration of Ca(OH)$_2$ particles from 30 to 900 °C under 100% N$_2$ atmosphere, (2) cooling step from 900 to 30 °C under 100% N$_2$ atmosphere and (3) carbonation experiment as explained above.

2.3. Gas–solid carbonation experiments under isothermal conditions

Experiments at six different temperatures (200, 300, 350, 400, 500, 600 °C) were performed to carbonate the Ca(OH)$_2$ in the thermogravimetric analyzer. About 3 min were necessary to reach the

reaction temperature and the flow of CO$_2$ was kept constant at 50 mL min^{-1} in all experiments. Note that 500 and 600 °C are critical temperatures because the Ca(OH)$_2$ particles are dehydroxylated in this temperature range. The in situ synthesized CaO was carbonated at 300, 600 and 800 °C. The in situ synthesis of CaO was carried out as follows: (1) dehydration of Ca(OH)$_2$ particles from 30 to 900 °C under 100% N$_2$ atmosphere, (2) cooling step from 900 to investigated temperature under 100% N$_2$ atmosphere and (3) isothermal carbonation of CaO at investigated temperature (300, 600 and 800 °C).

3. Results and discussion

The original results on dry gas–solid carbonation (relative humidity ≈ 0) of Ca(OH)$_2$ and CaO under non-isothermal and isothermal conditions are given below. Exclusively nanosized particles (<100 nm) of Ca(OH)$_2$ were used in the experiments. Moreover, an alternative reaction mechanism is proposed for gas–solid carbonation of Ca(OH)$_2$ at high temperature under dry conditions, i.e., when the relative humidity is close to zero (RH ≈ 0). This reaction mechanism was supported by the dry gas–solid carbonation of CaO particles synthesized in situ by complete dehydration of

Table 1
Summary of thermokinetic parameters for non-isothermal gas–solid carbonation of $Ca(OH)_2$ nanoparticles at three different constant heating rates.

H. rate (K/min)	Gaussian model 1st derivative vs. T			FWHM 2.3548σ	JMA model ξ vs. t		Augis and Bennett relation
	$a_{intensity}$ (1/s)	σ (K)	T_{max} (K)		k_A (1/s)	m	$E_a = \frac{2.5R(T_{max})^2}{m(FWHM)}$
5	1.92×10^{-4}	51.98	703.33	122.40	1.1456×10^{-4}	14.2	5.9159 kJ/mol
10	3.64×10^{-4}	54.16	712.66	127.53	2.2545×10^{-4}	13.9	5.955 kJ/mol
20	7.00×10^{-4}	59.54	722.13	140.20	7.0912×10^{-4}	6.67	11.5912 kJ/mol

T: temperature; 1st *derivative*: first derivative on TG curve; ξ: fractional carbonation extent; t: time; JMA: Johnson–Mehl–Avrami; H: heating; σ: standard deviation; $a_{intensity}$: intensity of peak; T_{max}: maximum value of peak; FWHM: full width at half maximum value of peak; k_A: kinetic constant; m: kinetic exponent; E_a: activation energy.

$Ca(OH)_2$ from 30 to 900 °C under N_2 atmosphere in the TG analyzer as described in Section 2.

3.1. Gas–solid carbonation of $Ca(OH)_2$ nanoparticles under non-isothermal conditions

Fig. 1 shows the gas–solid carbonation of $Ca(OH)_2$ nanoparticles under non-isothermal conditions at two different heating rates (5 and 10 K/min). In both cases, a high carbonation extent ($\xi = 0.94$) was obtained according to TG curves. Moreover, based on the 1st derivative curves (DTG) for the three heating rates, it may be concluded that the level of carbonation detected from 300 to about 550 K was insignificant. In this temperature range, the initial adsorbed water (slight amount 1–2%) was preferentially removed, indicating low or negative stability of molecular water on the $Ca(OH)_2$ surface when the temperature increased (drying process under 100% CO_2). Concerning the carbonation process, a first step of slight carbonation was suspected in a reduced temperature range (from 550 to about 590 K) followed by a second step of significant carbonation which takes place in a broad temperature range until an apparent equilibrium is reached (from 590 to about 900 K) (see Fig. 1). This second carbonation step presents a sigmoidal thermokinetic behavior pattern as attested by a simple fitting of experimental curves. This gas–solid carbonation of $Ca(OH)_2$ nanoparticles can be expressed by the following general chemical reaction:

$$Ca(OH)_{2(s)} + CO_{2(g)} \rightarrow CaCO_{3(s)} + H_2O_{(g)} \qquad (1)$$
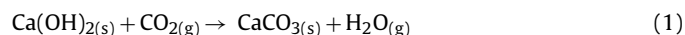
Under dry conditions, i.e., when relative humidity (RH) is close to 0 in the system, it was assumed that the molecular water produced from reaction (1) was simultaneously expelled with respected to the formed carbonate from reaction (1). In other words, the molecular water produced during carbonation is not stable in the carbonate–hydroxide interfaces and/or pores. This assumption is valid for small $Ca(OH)_2$ particles (<30 μm) as recently demonstrated by Blamey et al. (2011). However, another hypothesis was recently suggested by Materic et al. (2010, 2011), who claimed that $Ca(OH)_2$ particles present a higher thermal stability under a CO_2-rich atmosphere (termed by authors "superheated dehydration"), which prevents significant conversion to $CaCO_3$. Conversely, Blamey et al. (2011) have clearly demonstrated that the so-called superheated dehydration is absent for fine $Ca(OH)_2$ particles (<30 μm).

Various calculations were performed in order to estimate the activation energy for this gas–solid carbonation process (sigmoidal thermokinetic process in Fig. 1) by using a simple relation, originally proposed by Augis and Bennett (1978) in order to calculate conveniently the kinetic exponent m for the Johnson–Mehl–Avrami (JMA) model. In our study, the Augis and Bennett relation was used to calculate directly the activation energy (E_a) as follows:

$$E_a = \frac{2.5R(T_{max})^2}{m(FWHM)} \qquad (2)$$

where T_{max} is the maximum of the DTG peak related to sigmoidal thermokinetic behavior (see Fig. 1), FWHM is the full width at half maximum of the DTG peak, m is a kinetic exponent and R is the ideal gas constant (8.3144621 J/mol K). T_{max} and FWHM parameters were determined by using a classic Gaussian model; m was determined from the ξ vs. t experimental curve using the JMA model. All parameters and calculated activation energies for non-isothermal gas–solid carbonation of $Ca(OH)_2$ nanoparticles at three different heating rates are summarized in Table 1. A low activation energy (from 5.9 to 11.6 kJ/mol) is required to start the main carbonation step of $Ca(OH)_2$ particles at the three heating rates investigated. These estimated values are in agreement with the values reported by Nikulshina et al. (2007). In our study, a similar activation energy (about 6 kJ/mol) was determined in the experiments with 5 and 10 K/min heating rates. Conversely, a higher activation energy (about 12 kJ/mol) was determined at the 20 K/min rate. Based on these results, 10 K/min was considered as the optimized heating rate in our experiments.

As expected, the calcium carbonate ($CaCO_3$) formed in situ from reaction (1) remains stable at higher temperature under a 100% CO_2 atmosphere compared with the pure calcium carbonate (calcite) decomposed under inert 100% N_2 atmosphere (see Fig. 2). This was probably due to a simultaneous decarbonation–carbonation process at high temperature before a classic and complete decarbonation reaction ($CaCO_{3(s)} \rightarrow CaO_{(s)} + CO_{2(g)}$). In our study, the gas–solid carbonation of $Ca(OH)_2$ followed by the respective decarbonation of the carbonate formed (carbonation–calcination cycle under 100% CO_2) confirmed a complete carbonation process (ξ close to 1) through a simple mass balance. This means that the initial $Ca(OH)_2$ reactant was slightly carbonated (>3%); and the
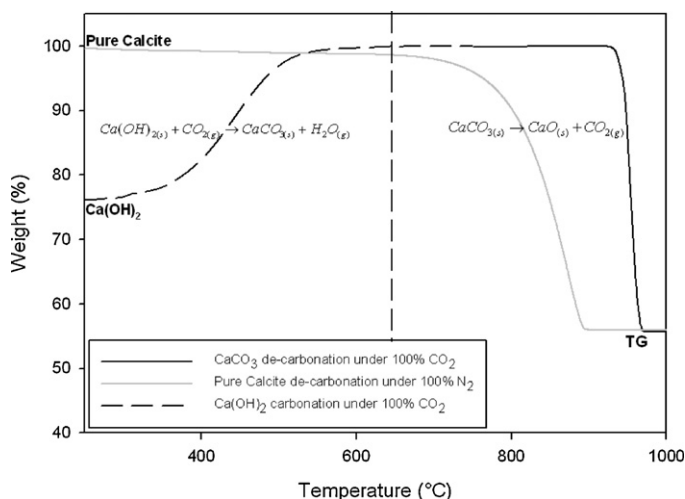

Fig. 2. Calcite decomposition (decarbonation) under 100% N_2 atmosphere compared with decarbonation of calcium carbonate under 100% CO_2 atmosphere. The latter was formed in situ from the gas–solid carbonation of $Ca(OH)_2$. The gas–solid carbonation of $Ca(OH)_2$ (dashed curve) was normalized to 100% in weight based on the decarbonation balance for the carbonate formed.

Table 2
Summary of kinetic parameters for isothermal gas–solid carbonation of $Ca(OH)_2$ nanoparticles at six different temperatures.

$T (^\circ C)$	Kinetic pseudo-second-order model: ξ_{iso} vs. t			v_0 (1/s)
	$\xi_{iso,max}$	$t_{1/2}$ (s)	R	
200	*Carbonation was not detected by TG*			
300	$0.1050 \pm 1 \times 10^{-4}$	3093 ± 14	0.98	3.3947×10^{-5}
350	$0.3948 \pm 7 \times 10^{-4}$	7169 ± 32	0.99	5.5070×10^{-5}
400	$0.5727 \pm 5 \times 10^{-4}$	2508 ± 10	0.99	2.2834×10^{-4}
500	$0.0780 \pm 6.85 \times 10^{-5}$	115 ± 3	0.80	6.7826×10^{-4}
600	$0.1318 \pm 5.13 \times 10^{-5}$	793 ± 35	0.99	1.6620×10^{-4}

ξ_{iso}: carbonation extent as a function of time t; $\xi_{iso,max}$: maximum value of carbonation extent at apparent equilibrium; $t_{1/2}$: the half-carbonation time; $v_0 = \xi_{iso,max}/t_{1/2}$: gas–solid carbonation rate.

mineralization of CO_2 did not form a protective carbonate layer around the reacting particles of $Ca(OH)_2$ as typically described in the literature (e.g., Sun et al., 2008; Chen et al., 2007; Fernandez Bertos et al., 2004). For this reason, the gas–solid carbonation of $Ca(OH)_2$ in Fig. 2 was normalized to 100%.

3.2. Gas–solid carbonation of $Ca(OH)_2$ nanoparticles under isothermal conditions

Our results clearly show that complete gas–solid carbonation of $Ca(OH)_2$ nanoparticles is never achieved under isothermal conditions for any of the investigated temperatures (200, 300, 350, 400, 500 and 600 °C) (see Fig. 3). It would appear that 400 °C is the optimized temperature, but the carbonation extent (ξ_{iso}) at this temperature reaches an apparent equilibrium value of only about 0.57 (w/w) (see Table 2). No gas–solid carbonation of $Ca(OH)_2$ was detected at 200 °C. Only a small carbonation extent (ξ_{iso} = 0.10, w/w) and a moderate extent (ξ_{iso} = 0.39, w/w) were determined at 300 and 350 °C, respectively. This is in agreement with the formation of a dense non-porous layer of carbonate mineral around the core of the reacting $Ca(OH)_2$ particles, leading to a passivation process as the intra-particle diffusion of CO_2 through the core of reacting particles is blocked, as explained in several studies (e.g., Montes-Hernandez et al., 2010a; Stendardo and Foscolo, 2009; Sun et al., 2008; Fernandez Bertos et al., 2004). Interpretation of the gas–solid carbonation at 500 and 600 °C is more complex. For these cases, there may be competition between $Ca(OH)_2$ dehydroxylation and gas–solid carbonation of CaO and $Ca(OH)_2$. For the sake of simplicity, the values of carbonation extent at 500 and 600 °C reported in Fig. 3 were normalized with the initial weight of $Ca(OH)_2$.
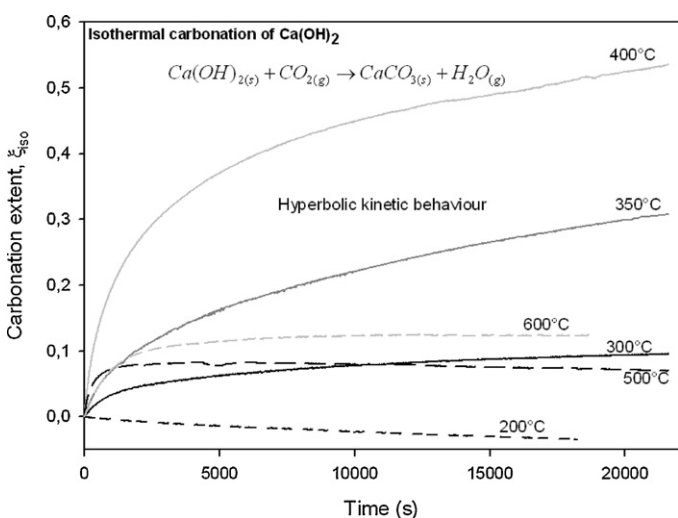
The experimental curves shown in Fig. 3 were fitted using a kinetic pseudo-second-order model. This model implies a fast carbonation step followed by a slow carbonation step. The latter was interpreted as a passivation step in our study. The integrated form of this kinetic model is given by the following hyperbolic equation:

$$\xi_{iso} = \frac{\xi_{iso,max} t}{t_{1/2} + t} \tag{3}$$

where ξ_{iso} is the carbonation extent as a function of time t under isothermal conditions, $\xi_{iso,max}$ is the maximum value of carbonation extent at apparent equilibrium and $t_{1/2}$ is the half-carbonation time, i.e., the time taken to achieve half the maximum value of carbonation extent. A non-linear regression by the least-squares method was performed to determine these kinetic parameters for each carbonation temperature. All values, including correlation factors and initial gas–solid carbonation rates ($v_0 = \xi_{iso,max}/t_{1/2}$) are summarized in Table 2. Arrhenius law (linear form) is frequently used to determine the apparent activation energy and frequency factor for isothermal processes. In our study, the carbonation temperatures 300, 350 and 400 °C revealed poor Arrhenius-type dependency (values not reported).

A simple comparison between non-isothermal and isothermal gas–solid carbonation of $Ca(OH)_2$ shows clearly that non-isothermal carbonation is faster and the reaction is complete (ξ close to 1) (see also Fig. 4). In other words, for isothermal carbonation, a non-porous carbonate layer is assumed to form around the reacting particles as typically described in the literature (e.g., Sun et al., 2008; Chen et al., 2007; Fernandez Bertos et al., 2004) while for non-isothermal carbonation, continuous $Ca(OH)_2$–$CaCO_3$

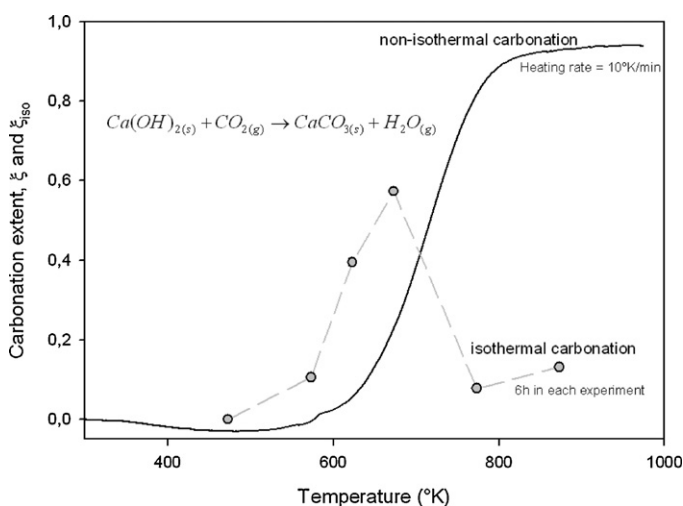**Fig. 3.** Gas–solid carbonation of $Ca(OH)_2$ under isothermal conditions for six different reaction temperatures.

Fig. 4. Comparison between gas–solid carbonation of $Ca(OH)_2$ under non-isothermal and isothermal conditions. For isothermal carbonation, the maximum values of carbonation extent for each reaction temperature were plotted.
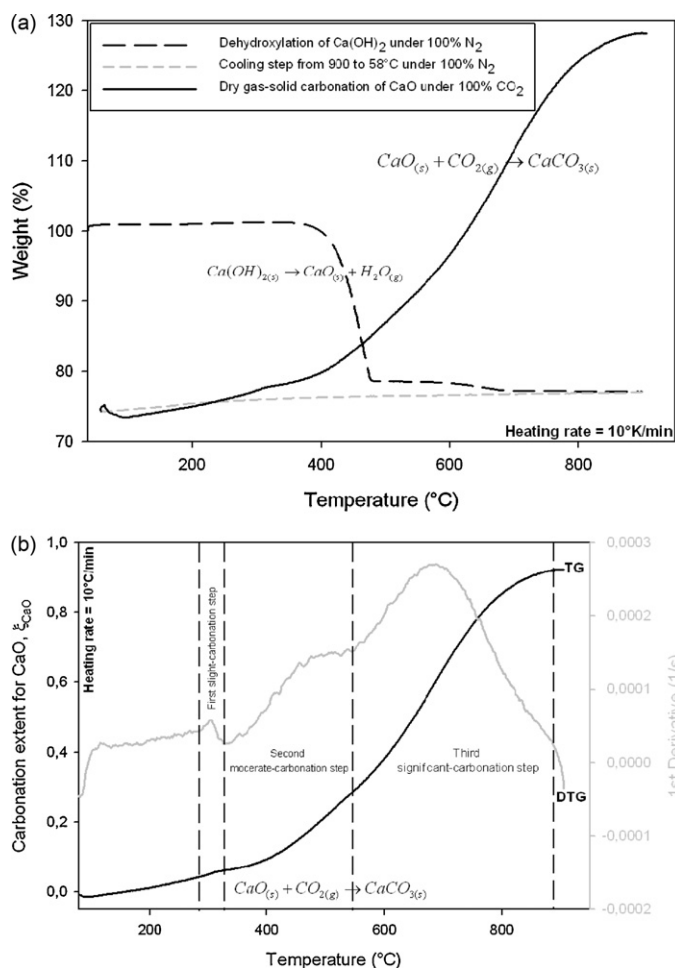
Fig. 6. Comparison between gas–solid carbonation of $Ca(OH)_2$ and CaO under non-isothermal conditions at the same heating rate (10 °C/min).

Fig. 5. (a) In situ synthesis and dry gas–solid carbonation of CaO particles under non-isothermal conditions at constant heating rate (10 °C/min). (b) Carbonation extent (ξ_{CaO}) was determined from thermogravimetric (TG) curve and differential thermogravimetric (DTG) curves were used for qualitative identification of the carbonation steps.

transformation takes place until completion of the reaction as shown by the decarbonation curves in Fig. 2.

3.3. Gas–solid carbonation of CaO vs. gas–solid carbonation of $Ca(OH)_2$: non-isothermal conditions

As shown in Fig. 5(a), the CaO particles were synthesized in situ by dehydroxylation of $Ca(OH)_2$ from 30 to 900 °C under 100% N_2 atmosphere followed by simple cooling of the CaO particles from 900 to 30 °C also under 100% N_2 atmosphere. Finally, the dry gas–solid carbonation of CaO with pure CO_2 (100% CO_2 atmosphere of 50 mL/min) was carried out using a heating rate of 10 °C/min. The dry gas–solid carbonation of CaO particles takes place in a broad temperature range (from 100 to 900 °C) and three main carbonation regimes or steps were qualitatively identified by plotting the first derivative curve (DTG) (see Fig. 5(b)). These carbonation steps were arbitrarily defined as slight, moderate and significant depending on the carbonation extent reached as a function of temperature. Unfortunately, the moderate and significant carbonation steps clearly overlapped, complicating the characterization of their peak values. For this reason, the relation (2) previously used to determine the activation energy of $Ca(OH)_2$ carbonation, was not directly applicable to CaO carbonation. On the other hand, a high carbonation extent was reached ($\xi_{CaO} = 0.92$) at the apparent equilibrium. Technically, this value was similar to the carbonation extent obtained

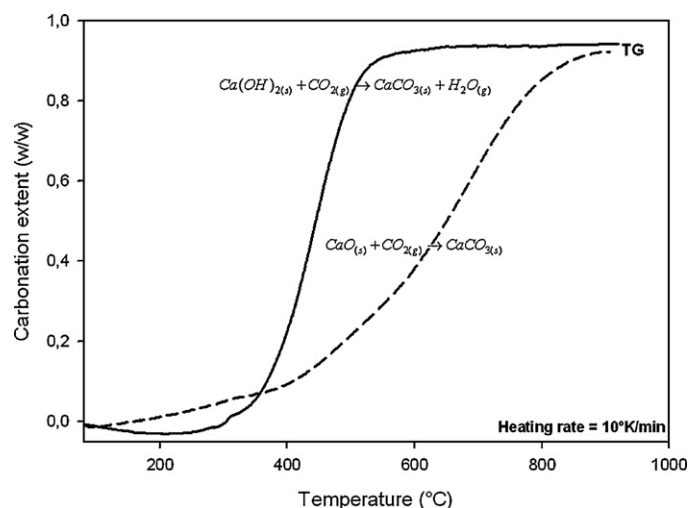for $Ca(OH)_2$ ($\xi = 0.94$) (see Fig. 6). Conversely, the gas–solid carbonation of CaO takes place in a broader temperature range, implying more complex thermokinetic behavior (overlapping of carbonation regimes). Based on these results, it is assumed that the simultaneous expelling of produced molecular water during gas–solid carbonation of $Ca(OH)_2$ (reaction (1)) could significantly enhance CO_2 transfer from the gas phase toward unreacted $Ca(OH)_2$ surfaces. In this way, micro-cracking produced by fast expelling of water vapor is suspected. Note that the fast and simultaneous expelling of produced molecular water during $Ca(OH)_2$ carbonation indicates that the CO_2 aqueous speciation at the $CaCO_3$–$Ca(OH)_2$ interfaces will be zero and/or insignificant at high temperature (>300 °C) and preferential for small $Ca(OH)_2$ particles (<30 μm). This assumption is in agreement with recent results reported by Blamey et al. (2011).

3.4. Dry gas–solid carbonation of CaO particles under isothermal conditions

The CaO particles were synthesized in situ by dehydroxylation of $Ca(OH)_2$ from 30 to 900 °C under 100% N_2 atmosphere followed by simple cooling of CaO particles from 900 to 800 °C also under 100% N_2 atmosphere (similar to Fig. 5(a)). Finally, dry gas–solid carbonation of CaO with pure CO_2 (100% CO_2 atmosphere of 50 mL/min) was carried out at constant temperature (300, 600 or 800 °C). A very low carbonation extent was found at 300 °C (<0.1) and similar high-carbonation extents were found at 600 °C and 800 °C. High temperature (>600 °C) promotes a high-carbonation extent, probably due to the fact that this temperature is close to the decarbonation temperature of the actual carbonate formed (see Fig. 2). Concerning the gas–solid carbonation of CaO particles at 800 °C, a small difference was found between two independent carbonation experiments after 4–6 h of carbonation reaction. This small difference can only be related to the initial weight (not strictly controlled) (see Fig. 7). In this case, a high carbonation extent ($\xi_{iso\text{-}CaO} = 0.91$) was reached after 6 h of reaction, but the apparent equilibrium had still not been reached. A kinetic model can be used to predict the apparent equilibrium with respect to the maximum value of carbonation extent. A simple non-linear regression using Eq. (3) (kinetic pseudo-second-order model) does not provide sufficient correlation with experimental kinetic data. For this reason, the kinetic experimental data were fitted using a kinetic double-pseudo-second-order model. This model assumes two kinetic regimes due to the presence of two types of reactive
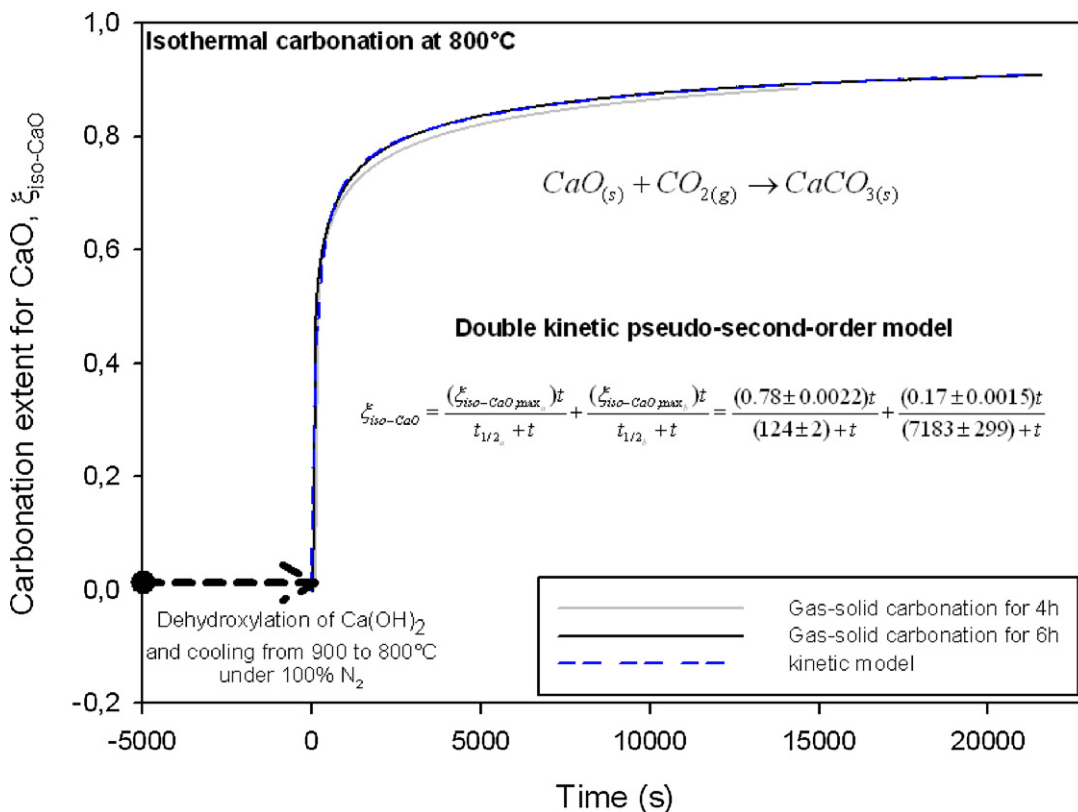
Fig. 7. Gas–solid carbonation of in situ synthesized CaO under isothermal conditions (800 °C) after 4 and 6 h reaction time. Experimental curve (6 h reaction time) was fitted using a double kinetic pseudo-second-order model.

surface sites. Its integrated form is given by the following hyperbolic equation:

$$\xi_{iso\text{-}CaO} = \frac{(\xi_{iso\text{-}CaO,max_a})t}{t_{1/2_a} + t} + \frac{(\xi_{iso\text{-}CaO,max_b})t}{t_{1/2_b} + t} \qquad (4)$$

where $\xi_{iso\text{-}CaO}$ is the carbonation extent as a function of time t under isothermal conditions, $\xi_{iso\text{-}CaO,max_a}$ and $\xi_{iso\text{-}CaO,max_b}$ are the maximum values of carbonation extent at apparent equilibrium for each kinetic regime and $t_{1/2_a}$ and $t_{1/2_b}$ are the half-carbonation times, i.e., the time taken to achieve half of the maximum value of carbonation extent for each kinetic regime. A non-linear regression by the least-squares method was performed to determine these kinetic parameters for each carbonation temperature. All values, including estimated errors are directly reported in Fig. 7. The predicted total carbonation extent ($\xi_{iso\text{-}CaO,max_{total}} = \xi_{iso\text{-}CaO,max_a} + \xi_{iso\text{-}CaO,max_b} = 0.95$) reached at apparent equilibrium is similar to the CaO carbonation extent obtained under non-isothermal conditions. Moreover, two kinetic regimes were clearly identified, the first kinetic regime takes only a couple of minutes ($t_{1/2_a} = 124$ s) to be established; conversely, the second kinetic regime takes several hours ($t_{1/2_b} = 7183$ s).

As reported in Fig. 3, the highest gas–solid carbonation extent (about 0.57) was obtained for Ca(OH)$_2$ at 400 °C. This value is significantly lower than the carbonation extent (0.91) obtained from gas–solid carbonation of synthesized CaO at 800 °C, with a carbonation reaction duration of 6 h for both cases (see Fig. 8). The kinetic behavior was also found to differ for each case with a single kinetic pseudo-second-order model for the gas–solid carbonation of Ca(OH)$_2$ (one type of reactive surface site) and a double kinetic pseudo-second-order model for the gas–solid carbonation of CaO (two types of reactive surface site).

3.5. Reaction mechanism for dry gas–solid carbonation of Ca(OH)$_2$ and CaO

The reaction mechanism for carbonation of Ca(OH)$_2$ with a relative humidity (RH) > 0 has been successfully explained, assuming CO$_2$ dissociation in molecular water at the reacting interfaces (e.g., Montes-Hernandez et al., 2010b; Beruto and Botter, 2000). However, the gas–solid carbonation reaction of Ca(OH)$_2$ at low temperature (30 °C) and low CO$_2$ pressure (<2 bar) was inhibited at RH ≈ 0 (Montes-Hernandez et al., 2010a). The dry gas–solid
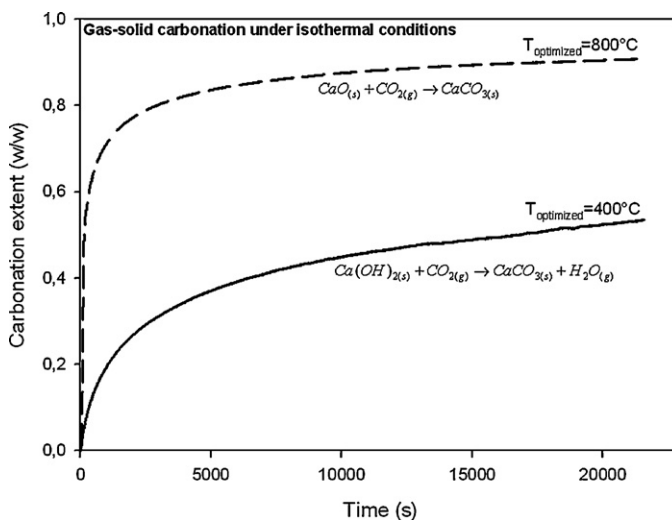

Fig. 8. Comparison between gas–solid carbonation of Ca(OH)$_2$ and CaO under isothermal conditions. Concerns only the optimized temperatures, 400 °C for Ca(OH)$_2$ carbonation and 800 °C for CaO carbonation.

carbonation of $Ca(OH)_2$ can be reactivated at high temperature (>200 °C). As mentioned above, the molecular water produced during the carbonation reaction of $Ca(OH)_2$ is not stable or is insignificantly stable on the reaction interfaces at high temperature, specially for small particles (<30 μm). This implies fast and simultaneous expelling of the molecular water produced. Based on these arguments, an alternative reaction mechanism is proposed for the gas–solid carbonation of $Ca(OH)_2$, when RH ≈ 0. In this alternative, it is assumed that atomic excitation at high temperature allows the local migration of one oxygen atom from the solid toward the adsorbed CO_2 leading to its mineralization into carbonate (porous or non-porous layer) around the reacting particles; chemically the mineralization of CO_2 also implies the breaking of one covalent bond in the CO_2 molecule. This simple reaction mechanism is also valid and clearly convincing for dry gas–solid carbonation (RH ≈ 0) of CaO particles because it does not involve the production of molecular water during the carbonation process.

$$CaO_{(s)} + CO_{2(g)} \rightarrow CaCO_{3(s)} \qquad (5)$$

The formation of complex carbonate ions (e.g., unidentate or bidentate carbonate) via chemisorption process is not excluded during carbonation process at high temperature as early proposed by Busca and Lorenzelli (1982) and Beruto et al. (1984).

4. Conclusion

In the present study, basic research was carried out to provide complementary insights into the gas–solid carbonation of $Ca(OH)_2$ and in situ synthesized CaO under non-isothermal and isothermal conditions. All carbonation experiments were carried out in a thermogravimetric analyzer. The results revealed that $Ca(OH)_2$-to-$CaCO_3$ and CaO-to-$CaCO_3$ solid state transformations are quasi-complete reactions under non-isothermal conditions when nanosized reacting particles are used. This means that CO_2 mineralization does lead to the formation of a protective carbonate layer around the reacting particles of $Ca(OH)_2$ and CaO. However, the formation of a protective carbonate layer around the reacting particles explains the incomplete carbonation under isothermal conditions, particularly for $Ca(OH)_2$.

Based on this experimental study, an alternative reaction mechanism is also proposed for the gas–solid carbonation of $Ca(OH)_2$, when the relative humidity is close to 0. In this alternative, it is assumed that the molecular water produced during the carbonation reaction of $Ca(OH)_2$ is not stable or is insignificantly stable on the reacting interfaces at high temperature, especially for small particles (<30 μm). This implies fast and simultaneous expelling of the molecular water produced. On the basis of these arguments it may be assumed that atomic excitation at high temperature allows the local migration of one oxygen atom from the solid toward the adsorbed CO_2 leading to its mineralization into carbonate (porous or non-porous layer) around the reacting particles. From a chemical standpoint, the mineralization of CO_2 also implies the breaking of one covalent bond in the CO_2 molecule. This simple reaction mechanism is also valid and clearly convincing for dry gas–solid carbonation (relative humidity ≈ 0) of CaO particles because it does not involve the production of molecular water during the carbonation process.

Acknowledgements

References

Augis, J.A., Bennett, J.E., 1978. Calculations of the Avrami parameters for heterogeneous solid state reaction using a medication of the Kissinger. Journal of Thermal Analysis 13, 283–292.

Beruto, D., Botter, R., Searcy, A., 1984. Thermodynamics and kinetics of carbon dioxide chemisorption on calcium oxide. Journal of Physical Chemistry 88, 4052–4055.

Beruto, D.T., Botter, R., 2000. Liquid-like H_2O adsorption layers to catalyse the $Ca(OH)_2$/CO_2 solid–gas reaction and to form a non-protective solid product layer at 20 °C. Journal of the European Ceramic Society 20, 497–503.

Blamey, J., Lu, D.Y., Fennell, P.S., Anthony, E., 2011. Reactivation of CaO-based sorbents for CO_2 capture: mechanism for the carbonation of $Ca(OH)_2$. Industrial & Engineering Chemistry Research 50, 10329–10334.

Busca, G., Lorenzelli, V., 1982. Infrared spectroscopic identification of species arising from reactive adsorption of carbon oxides on metal oxide surfaces. Materials Chemistry 7, 89–126.

Chen, M., Wang, N., Yu, J., Yamaguchi, A., 2007. Effects of porosity on carbonation and hydration resistance of CaO materials. Journal of the European Ceramic Society 27, 1953–1959.

Dheilly, R.M., Tudo, J., Sebai, Y., Queneudec, M., 2002. Influence of storage conditions on the carbonation of powdered $Ca(OH)_2$. Construction and Building Materials 16, 155–161.

Essaki, K., Kato, M., Uemoto, H., 2005. Influence of temperature and CO_2 concentration on the CO_2 absorption properties of lithium silicate pellets. Journal of Materials Science 21, 5017–5019.

Fernandez Bertos, M., Simons, S.J.R., Hills, C.D., Carey, P.J., 2004. A review of accelerated carbonation technology in the treatment of cement-based materials and sequestration. Journal of Hazardous Materials B112, 193–205.

Gauer, C., Heschel, W., 2006. Doped lithium orthosilicate for absorption of carbon dioxide. Journal of Materials Science 41, 2405–2409.

Huntzinger, D.N., Gierke, J.S., Kawatra, S.K., Eisele, T.C., Sutter, L.L., 2009. Carbon dioxide sequestration in cement kiln dust through mineral carbonation. Environmental Science & Technology 43, 1986–1992.

Lanas, J., Alvarez, J.I., 2004. Dolomitic limes: evolution of slaking process under different conditions. Thermochimica Acta 423, 1–12.

Larachi, F., Gravel, J.P., Grandjean, B.P.A., Beaudoin, G., 2012. Role of steam, hydrogen and pretreatment in chrysotile gas–solid carboantion: opportunities for pre-combustion CO_2 capture. International Journal of Greenhouse Gas Control 6, 69–76.

Materic, V., Edwards, S., Smedley, S.I., Holt, R., 2010. $Ca(OH)_2$ superheating as a low-attrition steam reactivation method for CaO in calcium looping applications. Industrial and Engineering Chemistry Research 49, 12429–12434.

Materic, V., Smedley, S.I., 2011. High temperature carbonation of $Ca(OH)_2$. Industrial & Engineering Chemistry Research 50, 5927–5932.

Montes-Hernandez, G., Daval, D., Chiriac, R., Renard, F., 2010a. Growth of nanosized calcite through gas–solid carbonation of nanosized portlandite particles under anisobaric conditions. Crystal Growth & Design 10, 4823–4830.

Montes-Hernandez, G., Daval, D., Findling, N., Chiriac, R., Renard, F., 2012. Linear growth rate of nanosized calcite synthesized via gas–solid carbonation of $Ca(OH)_2$ particles in a static bed reactor. Chemical Engineering Journal 180, 237–244.

Montes-Hernandez, G., Pommerol, A., Renard, F., Beck, P., Quirico, E., Brissaud, O., 2010b. In situ kinetic measurements of gas–solid carbonation of $Ca(OH)_2$ by using an infrared microscope coupled to a reaction cell. Chemical Engineering Journal 161, 250–256.

Nikulshina, V., Galvez, M.E., Steinfeld, A., 2007. Kinetic analysis of the carbonation reactions for capture of CO_2 from air via $Ca(OH)_2$–$CaCO_3$–CaO solar thermochemical cycle. Chemical Engineering Journal 129, 75–83.

Prigiobbe, V., Polettini, A., Baciocchi, R., 2009. Gas–solid carbonation kinetics of air pollution control residues for CO_2 storage. Chemical Engineering Journal 148, 270–278.

Purnell, P., Seneviratne, A.M.G., Short, N.R., Page, C.L., 2003. Super-critical carbonation of glass-fibre reinforced cement. Part 2: Microstructural observation. Composites: Part A 34, 1105–1112.

Rao, A., Anthony, E.J., Manovic, V., 2008. Sonochemical treatment of FBC ash: a study of the reaction mechanism and performance of synthetic sorbents. Fuel 87, 1927–1933.

Reddy, K.J., John, S., Weber, H., Argyle, M.D., Bhattachryya, P., Taylor, D.T., Christensen, M., Foulke, T., Fahlsing, P., 2011. Simultaneous capture and mineralization of coal combustion flue gas carbon dioxide (CO_2). Energy Procedia 4, 1574–1583.

Regnault, O., Lagneau, V., Schneider, H., 2009. Experimental measurement of portlandite carbonation kinetics with supercritical CO_2. Chemical Geology 265, 113–121.

Seo, Y., Jo, S.-H., Ryu, C.K., Yi, C.-K., 2007. Effects of water vapour pretreatment time and reaction temperature on CO_2 capture characteristics of a sodium-based solid sorbent in a bubbling fluidized-bed reactor. Chemosphere 69, 712–718.

Shtepenko, O.L., Hills, C.D., Coleman, N.J., Brough, A., 2005. Characterization and preliminary assessment of a sorbent produced by accelerated mineral carbonation. Environmental Science and Technology 39, 345–354.

Stendardo, S., Foscolo, P.U., 2009. Carbon dioxide capture with dolomite: a model for gas–solid reaction within the grains of a particulate sorbent. Chemical Engineering Science 64, 2343–2352.

Sun, P., Grace, J.R., Lim, C.J., Anthony, E.J., 2008. A discrete-pore-size-distribution-based gas–solid model and its application to the CaO+CO$_2$ reaction. Chemical Engineering Science 63, 57–70.

Wang, C., Jia, L., Tan, Y., Anthony, E.J., 2008. Carbonation of fly ash in oxy-fuel CFB combustion. Fuel 87, 1108–1114.

Zeman, F., 2008. Effect of steam hydration on performance of lime sorbent for CO$_2$ capture. International Journal of Greenhouse Gas Control 2, 203–209.

Zevenhoven, R., Teir, S., Eloneva, S., 2008. Heat optimisation of staged gas–solid mineral carbonation process for long-term CO$_2$ storage. Energy 33, 362–370.